Thermal Constriction Resistance Between Contacting Metallic Paraboloids: Application to Instrument Bearings

By

M. Michael Yovanovich

AIAA Paper No. 70-857 presented at the 5th Thermophysics Conference, Los Angeles, CA June 29 – July 1, 1970.

AIAA Progress in Astronautics and Aeronautics, Heat Transfer and Spacecraft Thermal Control, Vol. 24, 1971, Edited by John W. Lucas, pp. 337-358.

THERMAL CONSTRICTION RESISTANCE BETWEEN CONTACTING METALLIC PARABOLOIDS: APPLICATION TO INSTRUMENT BEARINGS

M. Michael Yovanovich*

University of Waterloo, Waterloo, Ont., Canada

In this paper the thermal constriction resistance between contacting paraboloids is considered, and the results of the theory are applied to the thermal analysis of a typical bearing element. In this analysis the complex thermal problem is resolved by the use of ellipsoidal coordinates which are intrinsic to both the shape of the contact area and the mixed boundary conditions: a) temperature prescribed over the contact which is isothermal and b) temperature gradient prescribed over the remainder of the contact plane which is impervious to heat transfer. An expression is developed for the total constriction resistance of a typical bearing element. The resistance is shown to be directly proportional to a geometric factor, which is a function of the ratio of the semimajor to semiminor axes, and inversely proportional to the product of the thermal conductivity and the semimajor axis. The theory is compared with test results, and the agreement is good.

Nomenclature

a = semimajor axis of elliptic contact area
A = constant
b = semiminor axis of elliptic contact area
B = constant
E = modulus of elasticity

Presented as Paper 70-857 at the AIAA 5th Thermophysics Conference, Los Angeles, Calif., June 29-July 1, 1970. Work performed at the Instrumentation Laboratory of Massachusetts Institute of Technology under NASA contract NAS9-6823. The author wishes to express his thanks to Arthur Grossman, Group Leader, Thermal Laboratory, Bedford Flight Facility; Ronald L. Morey; and Robert L. Henderson for their cooperation during all phases of this work.

*Associate Professor, Department of Mechanical Engineering.

F = force between contact solids
k = thermal conductivity
m = constant
n = constant
N = number of balls in a bearing
q = heat flux vector
Q = total heat flow
r = radial distance
R = thermal constriction resistance defined by Eq. (31)
T = temperature
α = contact angle
β = coefficient of expansion
ν = Poisson's ratio
Γ = contact area
Δ = coefficient defined by Eq. (3)
ρ = radius of curvature of contacting solids
ψ = constriction coefficient defined by Eq. (34)
ϕ = angle between planes containing principal curvatures

Subscripts

1,2 = solids 1 and 2, respectively, in contact
i,o = inner and outer races, respectively

Superscripts

unprimed = minimum radii of curvature
primed = maximum radii of curvature

Introduction

Many modern precision instruments are quite sensitive to temperature levels or temperature changes. When these electromechanical or optical instruments are mounted on gimbaled platforms, the total thermal resistance between the platform and the available thermal sink becomes very important. In a gimbaled system the instrument bearing will dominate the transfer of heat away from the source (the precision instruments). Since many systems operate in a vacuum, there are essentially two modes of heat transfer available: conduction through the solids and the metal-to-metal interfaces, and radiation across the gaps. For small temperature differences and low operating temperature levels the second mechanism will be small relative to the conduction mode.

A survey of the literature shows that only two studies[1,2] have dealt with the problem of heat transfer across a bearing. The first investigation[1] was experimental and showed the

magnitude of the thermal resistance of a typical bearing as a function of the bearing load and the influence of air and a lubricant upon the resistance. The investigator considered the case of a dry bearing in a vacuum, a dry bearing in air, as well as a lubricated bearing in a vacuum. He observed that a dry bearing in a vacuum offered from 10 to 5 times more resistance than the same dry bearing placed in air or the same lubricated bearing in a vacuum. The factor of 10 corresponds to a very light bearing load, while the factor of 5 corresponds to a higher bearing load (approximately 10 times the light load). In the first case the thermal resistance was dependent upon the applied load (approximately to the 1/3 power), while for the other two cases, the resistance was fairly independent of the load. The investigator[1] did not attempt an analysis of the thermal resistance, but did conclude that bearings different in size should have similar resistance if the number of balls is the same.

The second investigation[2] was analytical and showed which parameters were important and the influence of these parameters on the total resistance of the bearing. The analysis was based upon a symmetrically load bearing with heat flowing uniformly through each ball. The races were assumed to be flat and the contact areas were determined to be circular and very small relative to the radius of the balls. Assuming a particular thermal model, the investigator[2] showed that the total thermal resistance for a dry bearing in a vacuum is inversely proportional to the product of the number of balls, the radius of the contact area and the thermal conductivity of the balls. Since the contact area radius depends upon the ball radius, the material properties and the applied load, the effect of these parameters could be ascertained. The analysis showed that the resistance should vary as the load to the 1/3 power and is verified by the experimental results of the first investigation[1]. It was concluded that since both the inner and outer race of a bearing are not flat, but possess radii of curvature which can significantly influence the shape of the contact area which determines the magnitude of the thermal resistance, a more exact analysis should be performed to take into consideration the race curvatures.

An interface formed by the elastic contact of smooth solids (angular contact instrument bearing) will consist of a very large density of individual contacts which are said to comprise the contour area. For very smooth surfaces (roughness less than 5 μ in rms value) these small contacts (real contact area) will cover over 90% of the contour area. For such smooth surfaces it has been shown[3-5] that the total resistance can be predicted by considering the resistance due to the contour

area only. For this reason, no distinction will be made between the real and contour areas when considering the elastic contact and the thermal resistance.

In this paper it is assumed that heat transfer between contacing smooth paraboloids occurs through the contour area whose shape and size can be predicted by the Hertzian theory. The much more complex problem of heat transfer between contacting rough paraboloids will not be considered.

Elastic Contact Between Smooth Paraboloids

When two elastic solids having well-defined curved surfaces press against each other, an area of contact develops, the shape of which depends upon the principal curvatures of the surfaces near the point of contact, and the extent of which depends upon the force with which the solids press against each other. If the force is zero, the contact is a mathematical point. Whenever one solid exerts a force against another, an area of contact is formed which is generally elliptical. This area increases in size with increases in the force, but the shape remains invariant.

Since the shape and size of the contact area is of primary interest because the thermal constriction is a function of these contact area parameters, a few words will be said about the results of the Hertzian theory which predicts these parameters.

The complete Hertzian solution is available in standard texts on elasticity[6,7] and need not be repeated here. The solution must be evaluated in terms of elliptic integrals of the first and second kind. The semimajor and minor axes of the elliptic contact area are given by

$$a = m\,[(3\pi/4)F\,\Delta]^{1/3} \tag{1}$$

and

$$b = n\,[(3\pi/4)F\,\Delta]^{1/3} \tag{2}$$

in which

$$\Delta = \left(\frac{1-\nu_1^2}{\pi E_1} + \frac{1-\nu_2^2}{\pi E_2}\right)/(A+B) \tag{3}$$

The coefficients m and n are numbers depending on the ratio A/B (Fig. 1). A and B are determined from the following equations:

$$A + B = \frac{1}{2}\left(\frac{1}{\rho_1} + \frac{1}{\rho_1'} + \frac{1}{\rho_2} + \frac{1}{\rho_2'}\right) \tag{4}$$

and

$$B-A = \frac{1}{2}\left[\left(\frac{1}{\rho_1} - \frac{1}{\rho_1'}\right)^2 + \left(\frac{1}{\rho_2} - \frac{1}{\rho_2'}\right)^2 + 2\left(\frac{1}{\rho_1} - \frac{1}{\rho_1'}\right)\left(\frac{1}{\rho_2} - \frac{1}{\rho_2'}\right)\cos 2\phi\right]^{1/2} \tag{5}$$

The constants A and B of Eqs. (4) and (5) have the same sign.

Contact Between Sphere and Paraboloid

The expressions which depend upon the radii of curvature of the contacting solids can be reduced considerably when one of the solids is a sphere. Let us designate the paraboloid as solid 1 and the sphere as solid 2. Since the radii of curvature of the sphere are identical in all planes through its center, the angle ϕ can have any value. But this has no influence upon the results since the term 2ϕ in Eq. (5) is multiplied by $(1/\rho_2 - 1/\rho_2')$ which is zero. Thus Eqs. (4) and (5) simplify, for the paraboloid/sphere contact, to

$$A + B = \frac{1}{2}\left(\frac{1}{\rho_1} + \frac{1}{\rho_1'} + \frac{2}{\rho_2}\right) \tag{6}$$

and

$$B - A = \frac{1}{2}\left(\frac{1}{\rho_1} - \frac{1}{\rho_1'}\right) \tag{7}$$

If we first add Eqs. (6) and (7), we obtain an expression for A, and if we then subtract one from another, we get an expression for B. Taking the ratio of A to B we obtain

$$\frac{A}{B} = \frac{1/\rho_1' + 1/\rho_2}{1/\rho_1 + 1/\rho_2} \tag{8}$$

Contact Area Between Ball and Race

Since the curvatures of the inner and outer race are different (Fig. 2), the expressions for A+B and B/A, will therefore

differ for the ball/inner and ball/outer race combinations. For the inner race where ρ_i is negative and ρ'_i is positive, the expressions become

$$A + B = \frac{1}{2}\left(-\frac{1}{\rho_i} + \frac{1}{\rho'_i} + \frac{2}{\rho_2}\right) \tag{9}$$

and

$$\frac{A}{B} = \frac{1/\rho'_i + 1/\rho_2}{-1/\rho_i + 1/\rho_2} \tag{10}$$

At the outer race where both ρ_o and ρ'_o are negative, the expressions become

$$A + B = \frac{1}{2}\left(-\frac{1}{\rho_o} - \frac{1}{\rho'_o} + \frac{2}{\rho_2}\right) \tag{11}$$

and

$$\frac{A}{B} = \frac{-1/\rho'_o + 1/\rho_2}{-1/\rho_o + 1/\rho_2} \tag{12}$$

Illustrative Example

Consider as an example a bearing consisting of an inner and outer race, 42 spherical balls of 3/16 in diameter. All parts are fabricated from 440C stainless steel. The minimum radius of curvature of both the inner and outer race is 52% of the ball diameter. The maximum curvatures of both inner and outer race are 49/16 and 62/16 in, respectively. The physical characteristics of races and balls are $\nu_1 = \nu_2 = 0.25$ and $E_1 = E_2 = 29{,}000{,}000$ psi. It can be readily determined that for these two types of contacts the principal characteristics are as shown in Table 1.

Table 1 Bearing Geometric Characteristics

	Inner race	Outer race
A + B	5.825	5.24
A/B	30.0	27.4
m	3.37	3.25
m/n	8.70	8.20
Δ	$3.54 \times 10^{-2} B^{1/3}$	$3.94 \times 10^{-2} B^{1/3}$
a	0.68×10^{-9}	0.71×10^{-9}

It will be noted that there is only four % difference between the linear dimensions of the elliptic contact area at the inner and outer race. Consider the smaller of the two values as being typical of the contact area. For a bearing load of 17.3 lbs/ball the semimajor axis is $a = 1.84 \times 10^{-2}$ in and the semiminor axis b will be 8.70 times smaller. Thus the contact area is very small relative to the characteristic dimensions of the ball or races.

Thermal Model

As discussed in the previous section, the contact area between two smooth elastic paraboloids is always elliptic and it was shown that the semimajor and minor axes of the elliptic contact are quite small relative to the characteristic dimensions of the contacting solids. In the light of these facts it is assumed that the heat flow pattern in either solid will be fairly symmetrical about the contact plane, and thus it can be argued that the contact area is isothermal. The following discussion will be limited to the determination of the thermal constriction resistance when all the heat flows between the solids via the elliptic contact, i.e., there is no heat flow across the contact plane outside the contact area. This means that the surfaces of the contacting solids are adiabatic outside the contact area.

It is assumed that one half of the thermal constriction resistance problem can be adequately represented by an isolated, isothermal area either supplying or receiving heat from an other-wise insulated conducting half-space of thermal conductivity $k_{1,2}$ It is necessary to obtain a solution for Laplace's equation, $\nabla^2 T = 0$, in the half-space, $z > 0$, subject to the boundary conditions

$$T(x,y) = T_o \quad \text{in } \Gamma \tag{13}$$

and

$$[\partial T(x,y,z)/\partial z]_{z=0} = 0 \quad \text{outside } \Gamma \tag{14}$$

These equations form a so-called "mixed" boundary condition over the surface of the half space, $z > 0$, i.e., a temperature condition over the contact area and a temperature gradient condition over the rest of the surface. In general such boundary conditions are difficult to satisfy by means of simple functions, and this problem is even more difficult because of the shape of the contact area.

The boundary conditions on z = 0 are mixed, Eqs. (13) and (14) and not amenable to solution unless ellipsoidal coordinates are used. In ellipsoidal coordinates the Laplace equation becomes [5,8]

$$\nabla^2 T = \partial/\partial\lambda \left[\sqrt{f(\lambda)}\ (\partial T/\partial\lambda)\right] = 0 \tag{15}$$

where

$$\sqrt{f(\lambda)} = \sqrt{(a^2 + \lambda)(b^2 + \lambda)\lambda} \tag{16}$$

and a, b are the semimajor and semiminor axes, respectively, of the elliptic contact area.

The boundary conditions corresponding to Eqs. (13) and (14) are

$$\lambda = 0, \qquad T = T_o, \text{ constant} \tag{17}$$

$$\lambda \to \infty, \qquad T \to 0 \tag{18}$$

The Dirichlet problem in ellipsoidal coordinates automatically satisfies the mixed boundary value problem in Cartesian coordinates.

Integrating Eq. (15) twice we obtain as solution

$$T = A \int_o^\lambda \frac{d\lambda}{\sqrt{f(\lambda)}} + B^1 \tag{19}$$

where A and B^1 are constants of integration.

Equation (19) can be written as

$$T = A \left\{ \int_o^\infty \frac{d\lambda}{\sqrt{f(\lambda)}} - \int_\lambda^\infty \frac{d\lambda}{\sqrt{f(\lambda)}} \right\} + B^1 \tag{20}$$

where the integral from zero to infinity is constant. Writing

$$B = B^1 + A \int_\lambda^\infty \frac{d\lambda}{\sqrt{f(\lambda)}} \tag{21}$$

the solution becomes

$$T = B - A \int_{\lambda}^{\infty} \frac{d\lambda}{\sqrt{f(\lambda)}} \tag{22}$$

The boundary condition at infinity requires that B = 0 and the Dirichlet boundary condition over the elliptic area requires that we put

$$-A = \frac{T_o}{\int_o^{\infty} \frac{d\lambda}{\sqrt{f(\lambda)}}} \tag{23}$$

The temperature distribution in the half-space can now be written as

$$\frac{T}{T_o} = \frac{\int_{\lambda}^{\infty} \frac{d\lambda}{\sqrt{f(\lambda)}}}{\int_o^{\infty} \frac{d\lambda}{\sqrt{f(\lambda)}}} \tag{24}$$

The heat flux[5,8] is

$$q_{\lambda} = \frac{-k\, 2\sqrt{f(\lambda)}}{[(\lambda - \mu)(\lambda - \nu)]^{1/2}} \frac{\partial T}{\partial \lambda} \tag{25}$$

and upon taking the derivative of Eq. (24) with respect to λ and substituting into Eq. (25) we get

$$q_{\lambda} = \frac{2\, k\, T_o}{\int_o^{\infty} \frac{d\lambda}{\sqrt{f(\lambda)}}} \frac{1}{[(\lambda - \mu)(\lambda - \nu)]^{1/2}} \tag{26}$$

Equation (26) reduces to

$$q_{\lambda} = \frac{2\, k\, T_o}{r^2 \int_o^{\infty} \frac{d\lambda}{\sqrt{f(\lambda)}}} \tag{27}$$

for $\lambda \to \infty$ because $\lambda \to r^2$, and $\lambda >> \mu$ and $\lambda >> \nu$. At large distances from the elliptic area, the heat flux is practically radial and therefore one can write

$$q_\lambda = \frac{2\,k\,T_o}{r^2 \int_o^\infty \frac{d\lambda}{\sqrt{f(\lambda)}}} \doteq q_r = \frac{Q}{2\pi r^2} \tag{28}$$

The temperature distribution now becomes

$$T = \frac{Q}{4\pi k} \int_\lambda^\infty \frac{d\lambda}{\sqrt{f(\lambda)}} \tag{29}$$

and by the definition of thermal constriction resistance

$$R = [T_o - T(\lambda \to \infty)]/Q \tag{30}$$

we have

$$R = \frac{1}{4\pi k} \int_o^\infty \frac{d\lambda}{\sqrt{(a^2 + \lambda)(b^2 + \lambda)\lambda}} \tag{31}$$

Holm[9] has shown that Eq. (31) can be transformed into an equivalent form

$$R = \psi/4ka \tag{32}$$

where

$$\psi = \frac{2}{\pi} \int_o^{\pi/2} \frac{d\theta}{\{1 - \kappa^2 \sin^2 \theta\}^{1/2}} \tag{33}$$

and $\kappa^2 = 1 - b^2/a^2$.

k is the thermal conductivity of the half-space, a is the semi-major axis of the elliptic contact and ψ is a geometric factor depending upon the size of the contact. This geometric factor can be written as

$$\psi = \frac{2}{\pi} K \tag{34}$$

where K is the complete integral of the first kind of modulus $\kappa^2 = 1 - b^2/a^2$.

Equation (33) can be expanded and integrated term by term to yield the following useful expression:

$$\psi = 1 + \left(\frac{1}{2}\right)^2 \kappa^2 + \left(\frac{1.3}{2.4}\right)^2 \kappa^4 + \left(\frac{1.3.5}{2.4.6}\right)^2 \kappa^6 + \ldots + \left[\frac{(2n)!}{2^{2n}(n!)^2}\right]^2 \kappa^{2n} \quad (35)$$

Table 2 Typical Values of Geometric Factor ψ

a/b	ψ	a/b	ψ
1.0	1.000	6.0	2.030
1.5	1.212	6.5	2.082
2.0	1.372	7.0	2.136
2.5	1.402	7.5	2.172
3.0	1.610	8.0	2.214
3.5	1.702	8.5	2.252
4.0	1.784	9.0	2.286
4.5	1.856	9.5	2.322
5.0	1.920	10.0	2.352
5.5	1.980		

Thermal Constriction of a Typical Element

We can now determine the thermal constriction resistance of a typical bearing element (Fig. 2). We will make the analysis general by assuming that the thermal conductivities of the races differ from that of the balls. When all the heat flows from the inner to the outer race via the balls, there will be a constriction resistance at the inner race/ball contact as well as the outer race/ball contact. Thus the total resistance at the inner race/ball contact is

$$R_i = \psi_i / 4k_1 a_i + \psi_i / 4k_2 a_i \quad (36)$$

where k_1 and k_2 are the thermal conductivities of the inner race and ball, respectively. The constriction factor ψ_i is taken to be the same because of symmetry. A similar argument for the outer race/ball contact allows us to write the resistance as

$$R_o = \psi_o / 4k_3 a_o + \psi_o / 4k_2 a_o \quad (37)$$

The total constriction resistance of a typical bearing element is the sum of Eqs. (36) and (37)

$$R = \frac{\psi_i}{4k_1 a_i} + \frac{\psi_o}{4k_3 a_o} + \frac{1}{4k_2}\left(\frac{\psi_i}{a_i} + \frac{\psi_o}{a_o}\right) \quad (38)$$

For most bearings the linear dimensions of the elliptic contact areas at the inner and outer races are practically the same, i.e., $a_i = a_o$, and, therefore, $\psi_i = \psi_o$. Also the balls and races are usually fabricated from the same material so that $k_1 = k_2 = k$, and this permits us to write Eq. (38) as

$$R = \psi/ka \tag{39}$$

Thermal Resistance of a Typical Bearing

The results of the elastic deformation and thermal constriction analyses will now be used to obtain an expression for the total constriction resistance of a typical bearing. When a bearing is uniformly loaded, each ball in the assembly supports the same unit load. This means that the contact area will be identical at each ball/race contact. Since there is only 4% difference between the semimajor axes corresponding to the inner and outer races contacts, respectively, it will be assumed that ψ is the same for all contacts. Furthermore we will take the smaller value of ψ corresponding to the inner race contacts. larger

When the heat flow pattern through the bearing is uniform, we will assume that the constriction resistance is identical for each bearing element. This means that the total constriction of the bearing can be based upon the assumption that all the elements are thermally connected in parallel.

When these conditions of uniform loading and uniform heat flow are satisfied, the total constriction resistance becomes

$$R_b = \psi/Nka \tag{40}$$

where N is the total number of balls in the bearing. Upon substitution of Eq. (1) into the expression for the total constriction resistance we get

F = total axial load.

$$R_b = \frac{\psi(m/n)}{k\, m\, N^{2/3}\, [(3\pi/4)\Delta]^{1/3}\, [\bar{F}/\sin\alpha]^{1/3}} \tag{41}$$

We note that Eq. (41) depends upon a number of geometric and physical parameters as well as the axial load. For a particular bearing specified by its principal radii of curvature, number of balls, Young's modulus and Poisson's ratio, the parameters m, n, ψ, N and Δ are fixed being independent of the applied load. This means that some of the parameters in Eq. (41) can be lumped together and treated as a bearing constant.

The bearing resistance can be rewritten in the following simple form:

$$R_b = C_1/k\ B^{1/3} \tag{42}$$

where $B = F/\sin\alpha$ and C_1 is given by

$$C_1 = \frac{\psi(m/n)}{m\ N^{2/3}\ [(3\pi/4)\ \Delta]^{1/3}} \tag{43}$$

For the two bearings used in the test program the bearing constant C, is as shown in Table 3.

Table 3 Test Bearing Properties

Type	3TAR 33-42U	3TAR 49-62U
Bore, in.	2.0625	3.0625
OD, in.	2.6250	3.8750
Balls	44	42
Ball diameter, in.	1/8	3/16
Clearance, in.	0.0007-0.0012	0.0007-0.0012
Ball/race material, stainless steel	440C	440C
Young's modulus, psi	29×10^6	29×10^6
Coeff. of expansion, $1/^oF$	5.6×10^{-6}	5.6×10^{-6}
Hardness, Rockwell "C"	60-65	60-65
Thermal conductivity, BTU/HR FT^oF	13.8	13.8
C_1	1255	1130

The effect of applied load, bearing clearance, contact angle and thermal strains will be discussed in the following section utilizing the simple expression given by Eq. (42).

Factors Influencing the Bearing Load

There is a complex relationship between the axial load, the bearing load, the initial bearing clearance and the heat flow rate. The complex relationship arises from the thermal expansion of the balls and races because there is a temperature difference between the races, and the elastic compression of the balls and races. In other words, the clearance under load is equal to the initial clearance less the expansion due to thermal effects plus the displacement due to the elastic compression. With the aid of the nomenclature shown in Fig. 3, the relationship discussed above can be expressed in the following manner:

$$2(\rho_i' - \rho_2)(1 - \cos\alpha) = \delta_o - C_2\Delta T + \frac{C_3 F/\sin\alpha}{C_4 + C_5(F/\sin\alpha)^{2/3}} \quad (44)$$

The constants in Eq. (44) are given by[5,6]

$$C_2 = \beta(\rho_o' - \rho_2) \quad (45)$$

$$C_3 = \rho_i'/S_i + \rho_o'/S_o \quad (46)$$

$$C_4 = 2\pi E \quad (47)$$

$$C_5 = \frac{4}{\pi}\frac{C_\delta}{C_b}\left(\frac{N}{\Delta}\right)^{1/3}\left(\frac{1-\nu^2}{E}\right)\frac{1}{N} \quad (48)$$

The constants C_δ and C_b in Eq. (48) depend upon the principal radii of curvature through the geometric ratio A/B and values are found in Seely[6].

Equation (44) can be cast into a form which clearly shows the relationship between the axial load, the bearing load, heat flow and the initial bearing clearance. For the temperature difference in Eq. (44) write

$$\Delta T = QR_b = QC_1/B^{1/3} \quad (49)$$

Replace the contact angle dependence by writing

$$\cos\alpha = F/\sqrt{B^2 - F^2} \quad (50)$$

We now have

$$2(\rho_i' - \rho_2) = \delta_o - C_1C_2Q/B^{1/3} + C_3B/[C_4 + C_5B^{2/3}] \quad (51)$$

Knowing the initial clearance, Eq. (51) can be solved for B as a function of the heat flow rate Q after having solved Eqs. (43), (45-48) for the constants appearing in Eq. (51). The initial clearance is not known. The bearing manufacturer specifies a range of values for a typical bearing. Therefore, the best that one can do analytically is to solve Eq. (51) with δ_o as a parameter. Otherwise a series of experiments can be performed to determine the functional relationship between B, F, and Q.

Experimental Verification of the Theory

A systematic test program was conducted to obtain data which was compared with the values predicted by the theory. Two different sizes of angular contact instrument bearings were tested. Dry bearings were used and all tests were conducted in a vacuum of about 5×10^{-5} Torr. The test variables were the total axial load and the total heat flow rate. The experimental apparatus consisted of a vacuum chamber and vacuum pumps, a loading device, a heat source and heat sink, radiation shields and an instrument console.

A 15-watt (nominal) button heater was mounted on a copper block called the round centered hot block (Fig. 4). This hot block sat on the copper inner race. The interfaces between the hot block and keeper as well as the keeper and inner race were coated with Dow Corning 340 Silicone Heat Sink Compound. This insured that the heat path from the button heater to the inner race offered negligible thermal resistance. Thermocouples placed in the hot block and the keeper verified this. The outer race sat snuggly in the aluminum bearing support which stood on the base plate which acted as the heat sink. The base plate was cooled by a steady supply of city water. All interfaces were well greased with the heat sink compound. A 15-watt button heater was attached to an aluminum radiation shield which was placed under the inner race keeper (Fig. 4). This insured that all the heat from the source went to the inner race. Thermocouples were welded to the inner and outer race at diametrically opposite locations. They were also epoxied to insure that they would not be detached when handled.

The variable compression load on the bearing was supplied through a calibrated horseshoe-shaped force gauge mounted above the supermica insulating block. The insulating block completely enclosed the heater and rested on the hot block.

The bearings used in the tests were guaranteed by the supplier to be dry. They were kept away from oil and other contaminants when not being tested. All tests were performed with the bearings fixed in place and the total heat supplied by the button heater flowed from the inner to the outer race via the balls.

After mounting the test bearing, the chamber was pumped down to about 5×10^{-5} Torr. and these three procedures were followed to obtain the necessary data. In one test program, the load was fixed and the heat to the bearing was increased from

2.5 watts to a maximum of 15 watts in increments of 5 watts. In the second test program, the heat to the bearing was fixed while the total axial load was increased up to a maximum of about 500 lb. The third test program consisted of a mixture of load and heat flow changes from a minimum load and heat flow up to a maximum load and heat flow.

The outer race temperature varied from 70°F up to 81°F while the inner race temperature varied from 91°F up to a maximum of 245°F.

Correlation of Test Data and Discussion

The thermal resistance of a bearing given by Eq. (42) is not amenable to solution because the bearing load depends implicitly upon the temperature difference which is a function of the resistance. This can be seen by examining Eq. (44). If an initial bearing clearance of 0.001 in. is used in Eq. (44) or Eq. (51) one can determine the contact angle directly or the bearing load. Once these are known for a particular heat flow rate, then the thermal resistance can be calculated as a function of the axial load. The theory predicts values of the thermal resistance which show the same trend as the empirical data.

It was decided to use the second alternative described above to determine the relationship between B, F and Q. The results of the preliminary tests are shown in Figs. 5 and 6 where the bearing load is plotted against the axial load with heat flow as a parameter. At low axial loads the thermal expansion effect is important. Here it is seen that for a fixed axial load an increase in the heat flow results in an increase in the bearing load. This effectively reduces the thermal resistance. As the axial load increases, the effect of thermal expansion decreases. For loads above 600 lb the thermal effects are essentially negligible.

The relationship between bearing load and axial load as a function of heat flow rate was subsequently used to correlate all the experimental data obtained following the three procedures outlined in the previous section. There was excellent agreement between the experimental data and the predicted values of the resistance. This is clearly seen in Figs. 7 and 8. At low axial loads the resistance varies from a low value of about 10°F/watt up to a high value of about 22°F/watt for the 2.5-watt and 15-watt heat flow rates, respectively. The difference is due to thermal expansion effects as described above.

The thermal analysis was based upon the assumption that radiation effects are negligible. For the maximum temperatures observed (245-81) it is estimated that the thermal resistance due to radiation heat transfer would be about 300°F/watt. This is based upon the assumption that the inner race radiates directly to the outer race and both surfaces have emissivities of 0.8. The presence of the balls should increase the radiation resistance considerably. Thus the assumption of neglibible radiation transfer is valid for the low loads with temperature differences of 164°F and temperature levels of 245°F at the inner race. In the thermal analysis it was implicity assumed that all the resistance of a bearing can be attributed to the constriction of heat flow lines in the neighborhood of the contact areas at the ball/race interfaces. This in effect neglects the resistance to heat flow within the races and across the balls. The assumption used should become less true at high axial loads when the contact areas are large and the constriction resistances are small. In other words the thermal resistance through the races and balls, if important, should influence the total resistance at high axial loads. This was not observed and so it is concluded that this assumption is valid.

Conclusions

The analysis presented suggests that heat transfer through a bearing can be correlated extremely well provided that the surfaces are smooth, the contacts are formed elastically, the bearings are dry and placed in a vacuum, there is no radiation heat transfer across the gaps, and the bearing does not rotate. An expression for the total constriction resistance of a typical angular contact bearing is presented which shows that several physical and geometric parameters play a part in determining the resistance. It is also shown how thermal expansion and elastic compression of the balls and races influence the resistance. For a particular bearing having fixed geometric and physical characteristics, some of the parameters can be lumped together such that the bearing resistance can be correlated with the axial load and heat flow.

It is recommended that further work be done analytically and experimentally to determine the effects of lubricants, gases and rotation of the bearing.

References

[1]Jansson, R.M., "The Heat Transfer Properties of Structural Elements for Space Instruments, Report E-1173, Instrumentation

Laboratory, Massachusetts Institute of Technology, Cambridge, June 1962.

[2]Yovanovich, M.M., "Thermal Contact Resistance Across Elastically Deformed Spheres," Journal of Spacecraft and Rockets, Vol. 4, No. 1, Jan. 1967, pp. 119-122.

[3]Clausing, A.M. and Chao, B.T., "Thermal Contact Resistance in a Vacuum Environment," ASME Journal Heat Transfer, Vol. 87, May 1965, pp. 243-251.

[4]Yovanovich, M.M. and Rohsenow, W.M., "Influence of Surface Roughness and Waviness upon Thermal Contact Resistance," EPL Report 76361-48, June 1967, Mechanical Engineering Department, Mass. Inst. Technology.

[5]Yovanovich, M.M., "Analytical and Experimental Investigation of the Thermal Resistance of Angular Contact Instrument Bearings," Dec. 1967, Instrumentation Laboratory Report E-2215, Mass. Inst. Technology.

[6]Seely, F.B. and Smith, J.O., Advanced Mechanics of Materials, Wiley, New York, 1963, chap. 11.

[7]Love, A.E.H., Mathematical Theory of Elasticity, Dover, New York, 1944.

[8]Jeans, J.H., Mathematical Theory of Electricity and Magnetism, Cambridge University Press, Cambridge, 1963, pp. 244-245.

[9]Holm, R., Electric Contacts, Springer-Verlag, Berlin, 1958.

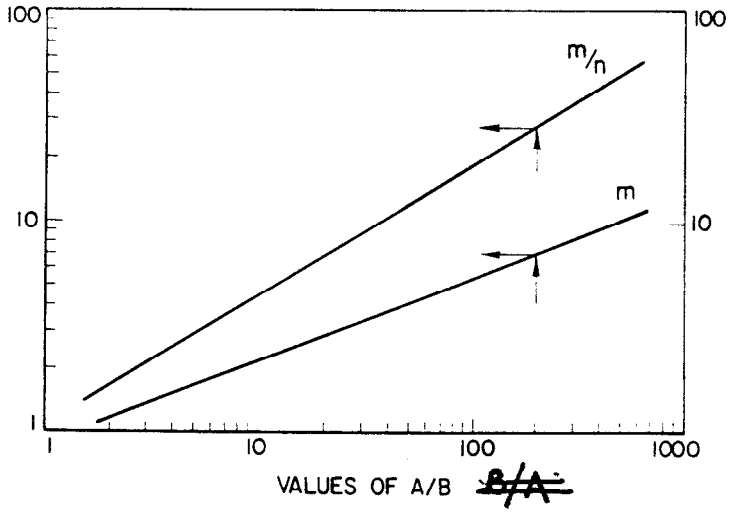

Fig. 1 Geometric parameters.

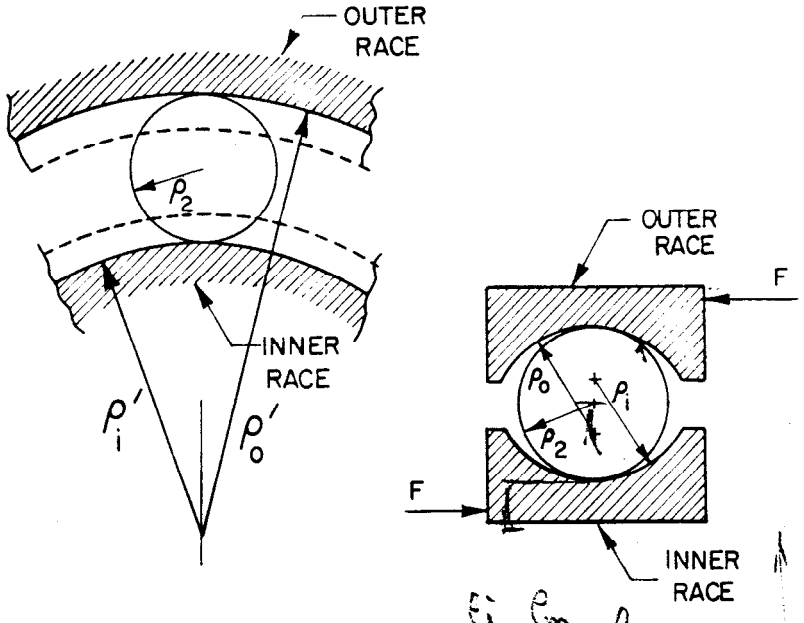

Fig. 2 Typical bearing element.

$D_m = \frac{1}{2}[D_i + D_o]$ $\rho_m = \frac{D_m}{2}$

$\rho_i = \rho_m - d/2 = \frac{D_m}{2} - \rho_2$

$\rho_o = \rho_m + d/2 = \frac{D_m}{2} + \rho_2$

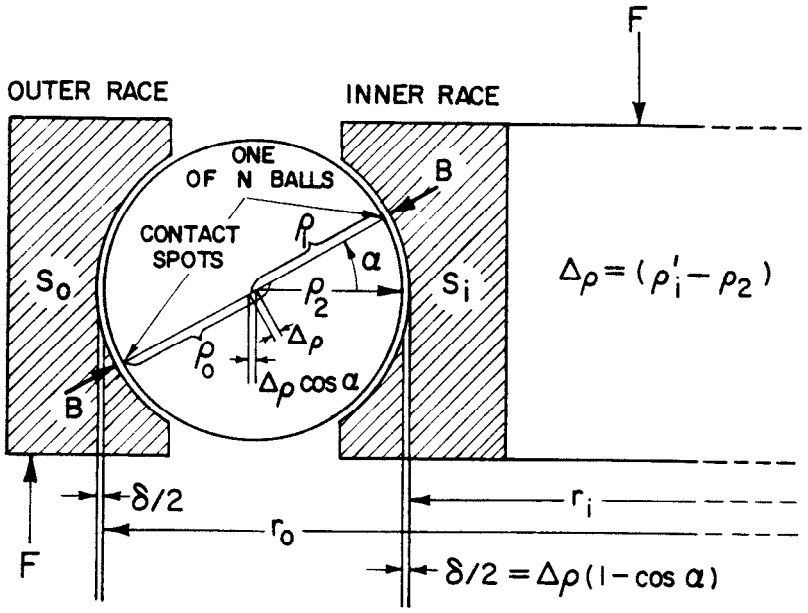

Fig. 3 Schematic of Ball and Races.

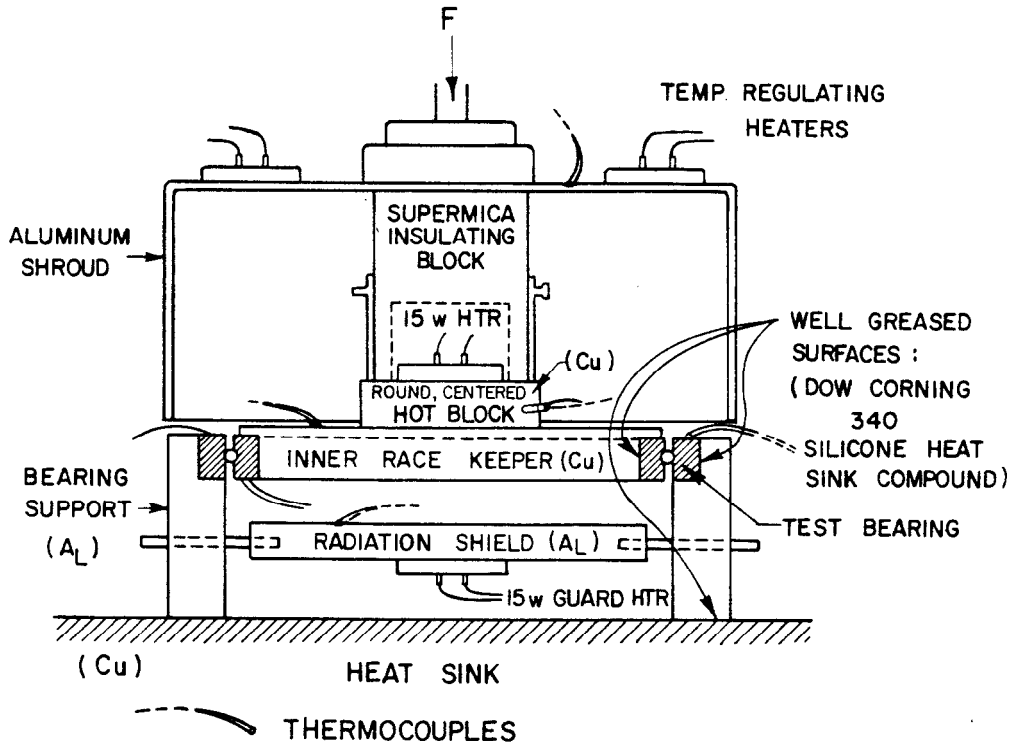

Fig. 4 Test apparatus.

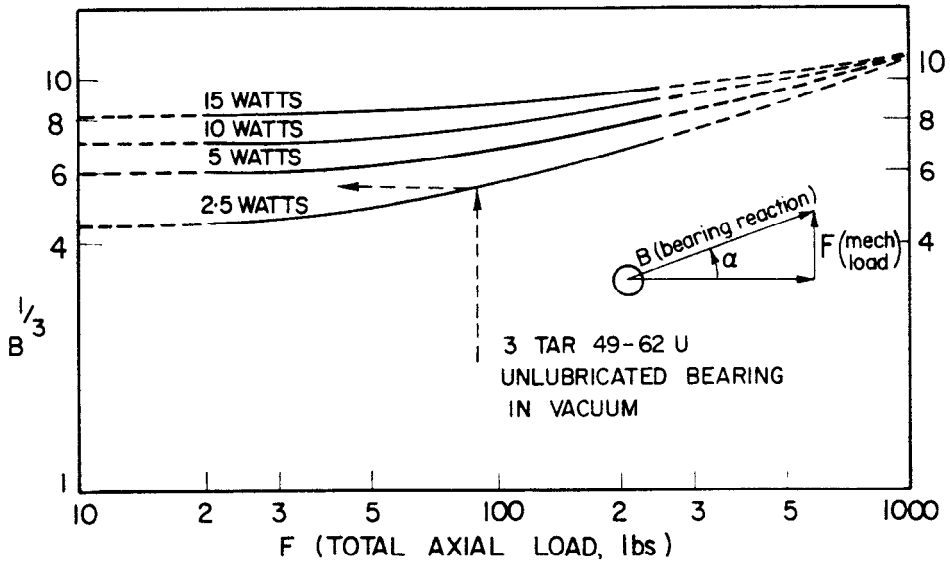

Fig. 5 Bearing load versus axial load.

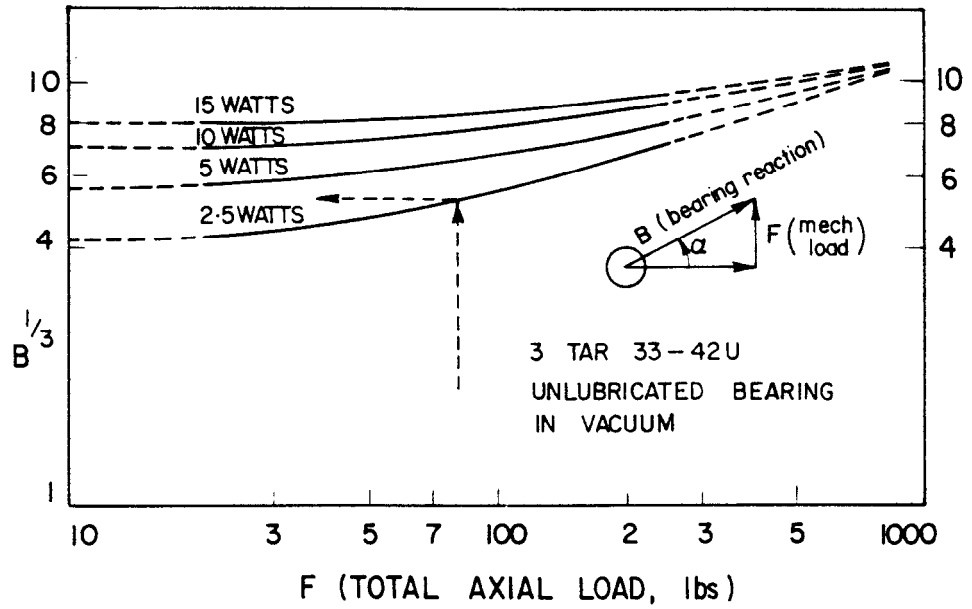

Fig. 6 Bearing load versus axial load.

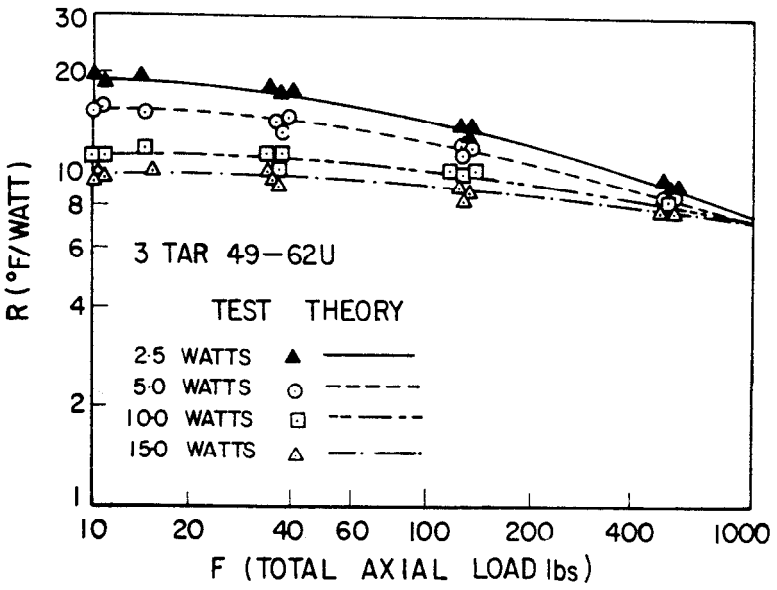

Fig. 7 Correlation of thermal resistance.

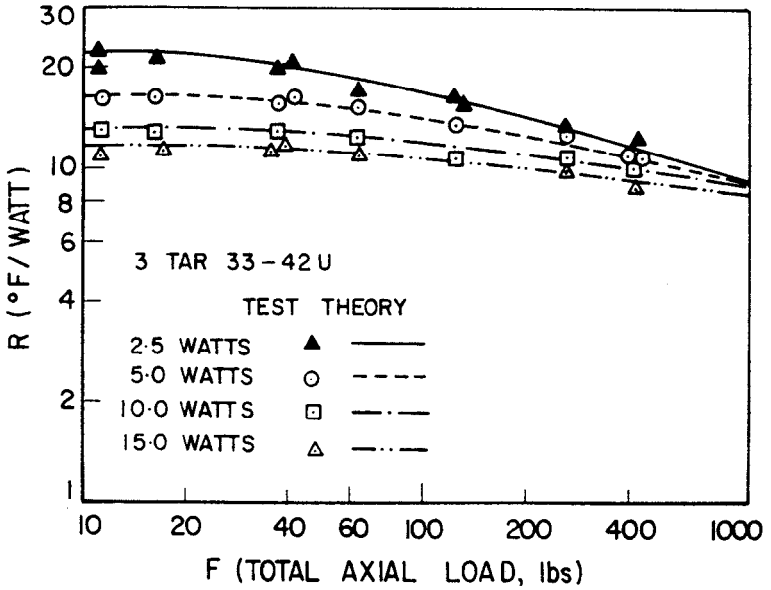

Fig. 8 Correlation of thermal resistance.